Effect of Sulfate Pretreatment on Gold-Modified TiO2 for Photocatalytic Applications

ARTICLE *in* THE JOURNAL OF PHYSICAL CHEMISTRY C · JULY 2009

Impact Factor: 4.77 · DOI: 10.1021/jp903432p

4 AUTHORS, INCLUDING:

M. Maicu
Technische Universität Dresden
10 PUBLICATIONS **451** CITATIONS
SEE PROFILE

G. Colón
Spanish National Research Council
131 PUBLICATIONS **4,569** CITATIONS
SEE PROFILE

Effect of Sulfate Pretreatment on Gold-Modified TiO_2 for Photocatalytic Applications

M. C. Hidalgo,* Marina Maicu, José A. Navío, and Gerardo Colón

Instituto de Ciencia de Materiales de Sevilla, Consejo Superior de Investigaciones Científicas (CSIC)y, Universidad de Sevilla, Americo Vespucio 49, 41092 Seville, Spain

Received: April 14, 2009; Revised Manuscript Received: June 1, 2009

The influence of sulfated pretreatment of TiO_2 on the structure, morphology, and dispersion of gold and photocatalytic properties of Au/TiO_2 were studied. Notable enhancements in the photocatalytic activity of TiO_2 were achieved by deposition of gold onto samples that had previously undergone sulfate treatment followed by high temperature calcination. The enhancement in activity can be attributed to the stronger bonding and improved electronic communication between gold particles and TiO_2 on defect rich surfaces as are found on sulfated samples after calcination at 700 °C. Two different methods for gold deposition were evaluated: chemical reduction by citrate and photodeposition. The citrate method produced more homogeneous and smaller gold particles with a better dispersion than photodeposition, which lead to greater increases in activity in the photocatalytic degradation of phenol when the former method was used for deposition on both sulfated and nonsulfated TiO_2. The combination of sulfate pretreatment and gold deposition by chemical reduction was shown to be a good strategy to obtain gold/titania catalysts possessing homogeneous particle size and dispersion of the metal and a strong bonding between the Au and the TiO_2 surface.

1. Introduction

Heterogeneous catalysis performed by gold nanoparticles supported on oxidic materials has been investigated in the last years for many different applications, including low temperature catalytic oxidation of CO[1,2] or propene,[3] water gas shift reactions,[4] or promotion of the photocatalytic activity of TiO_2.[5,6] The catalytic properties of Au/oxide catalysts are found to be highly dependent on the size and distribution of the gold nanoparticles and on interactions between the metal and the support.[7]

Focusing on photocatalytic applications, the addition of gold nanoparticles has been used to enhance the photoactivity of TiO_2, and the development of this strategy remains an important area of investigation within photocatalysis. Nanoparticles of gold and other noble metals deposited on the TiO_2 surface have been reported to increase the efficiency of the photocatalytic process by acting as electron sinks and decreasing the recombination rate of photogenerated charges.[5−10]

On the other hand, a synergetic increase in the photocatalytic activity of platinised TiO_2 which had been previously sulfated has been reported.[11] Pretreatment with sulfuric acid appears to stabilize TiO_2 surface area, preventing sintering and rutile crystalline phase formation until calcination temperatures as high as 700 °C. These materials have highly defective surfaces due to the dehydroxylation process of the excess of adsorbed protons during calcination.[12,13] Platinisation of presulfated TiO_2 surfaces lead to the formation of smaller and better dispersed platinum particles than in nonsulfated TiO_2, increasing at the same time the improvement of the photocatalytic activity.[11]

The work described here explores the effect of sulfate pretreatment of TiO_2 on gold-modified samples. Two different methods of gold deposition and different amounts of gold loadings were tested and the influence on the photocatalytic activity for phenol degradation was evaluated. A wide characterization of the samples was performed in order to elucidate the reasons for the different photocatalytic behavior between sulfated and nonsulfated Au/TiO_2 samples.

* Corresponding author. Tel: +34 954489550. Fax: +34 95 446 0665. E-mail: mchidalgo@icmse.csic.es.

2. Experimental Section

2.1. Catalyst Preparation. TiO_2 was prepared by a sol−gel method where the hydrolysis of titanium tetraisopropoxide (TTIP, Aldrich 97%) in isopropanol solution was achieved by the addition of distilled water (volume ratio TTIP/isopropanol/water 1:1:1). Afterward, the precipitate was filtered and dried at 110 °C overnight.

For the nonsulfated TiO_2, the dried precipitate was then simply calcined at 500 °C for 2 h. For the sulfated TiO_2, the dried precipitate was impregnated by a sulfuric acid 1 M solution for 1 h, then filtered again, dried at 110 °C overnight and calcined at 700 °C for 2 h. The differing calcination temperatures for the two different TiO_2 samples were selected in order to compare best samples in both series regarding photocatalytic activity for phenol degradation according to our previous work,[12] i.e., 500 °C for nonsulfated TiO_2 and 700 °C for sulfated TiO_2. However; for reference purposes, selected sulfated samples calcined at 500 °C and nonsulfated TiO_2 calcined at 700 °C were also prepared.

Gold was subsequently deposited on the surfaces via two different methods: photodeposition and chemical reduction by citrate.

The photodeposition of gold was performed over the calcined TiO_2 samples from gold(III) chloride solution ($HAuCl_4$ Sigma-Aldrich, 99.9+%) following a method previously described for the photodeposition of platinum.[11] Under an inert atmosphere, a suspension of TiO_2 in distilled water (5 g TiO_2 L^{-1}) containing isopropanol 0.3 M, which acts as sacrificial agent, and the appropriate concentration of $HAuCl_4$ depending on the required gold loading (0.5−1.5% weight total to TiO_2) was prepared. Photodeposition of gold was performed by illuminating the suspensions for 6 h with a medium pressure mercury lamp (400 W) of photon flux ca. 2.6×10^{-7} Einstein s^{-1} L^{-1} in the region

10.1021/jp903432p CCC: $40.75
Published on Web 06/18/2009

of wavelengths <400 nm. The powders were recovered by filtration and dried at 110 °C overnight.

Chemical reduction of gold was carried out by using sodium citrate as both reducing and stabilizing agent following another procedure described in the literature.[14] Appropriate amounts of $HAuCl_4$ for nominal contents of deposited Au between 0.5−1.5% weight total to TiO_2 were dissolved in distilled water (1 mg $HAuCl_4$/10 mL water). Then, suspensions of the different TiO_2 samples (1 g) in sodium citrate solutions (0.2 g/10 mL distilled water) were added. The finals suspensions were heated to reflux for 1 h under N_2 atmosphere to avoid gold reoxidation. After this time, the powders were washed, filtered and dried at 110 °C overnight.

To ensure that the preparatory methods gave reproducible results, selected samples were independently prepared and analyzed twice. Identical structural and morphological qualities and activities were observed in all cases.

Hereafter samples will be denoted by TiO_2 or S-TiO_2 (nonsulfated and sulfated respectively) followed by the weight % gold loading on the sample and an indication for the method used for gold deposition (*PD* for photodeposition and *Cit* for citrate method); e.g., S-TiO_2 1.5Au Cit means sulfated TiO_2 with 1.5 wt % nominal content of gold prepared by the citrate method.

2.2. Characterization of the Catalysts. Crystalline phase composition and degree of crystallinity of the samples were determined by X-ray diffraction (XRD). XRD patterns were obtained on a Siemens D-501 diffractometer with Ni filter and graphite monochromator using Cu Kα radiation (λ=1.5418 Å). Crystallite sizes in the different phases were estimated from the line broadening of the corresponding X-ray diffraction peaks by using the Scherrer equation. Peaks were fitted by using a Voigt function.

Transmission electron microscopy (TEM) and scanning electron microscopy (SEM) were used to study the morphology of the samples and the dispersion and size of the Au deposits. TEM was carried out using a Philips CM 200 instrument. The microscope was equipped with a top-entry holder and ion pumping system, operating at 200 kV and giving a nominal structural resolution of 0.21 nm. Field Emission SEM images were obtained in a Hitachi S-4800 microscope. For both TEM and SEM measurements, the samples were dispersed in ethanol using ultrasound and dropped on a carbon grid.

Surface characterization by X-ray photoelectron spectroscopy (XPS) was conducted on a Leybold-Heraeus LHS-10 spectrometer, working with constant pass energy of 50 eV. The spectrometer main chamber, working at a pressure $<2 \times 10^{-9}$ Torr, was equipped with an EA-200 MCD hemispherical electron analyzer with a dual X-ray source working with Al Kα ($h\nu$ = 1486.6 eV) at 120 W and 30 mA. The carbon 1s signal (284.6 eV) was used as the internal energy reference in all the experiments. Samples were outgassed in the prechamber of the instrument at 150 °C up to a pressure $<2 \times 10^{-8}$ Torr to remove chemisorbed water from their surfaces.

Total gold content of the samples was determined by X-ray fluorescence spectrometry (XRF) in a Panalytical Axios sequential spectrophotometer equipped with a rhodium tube as the source of radiation. XRF measurements were performed on pressed pellets (sample included in 10 wt % of wax).

BET surface area and porosity measurements were carried out by N_2 adsorption at 77 K using a Micromeritics ASAP 2010 instrument.

Light absorption properties of the samples were studied by UV−vis spectroscopy. UV−vis spectra were measured on a Varian Cary 100 spectrometer equipped with an integrating sphere with $BaSO_4$ as reference. Both absorbance and diffuse reflectance spectra were recorded for all samples and the Kubelka−Munk function, F(R∞), was applied to ensure a magnitude proportional to the extinction coefficient. Band-gaps were calculated through the Kubelka−Munk function, following the method proposed by Tandom and Gupta.[15]

2.3. Photocatalytic Runs. The photocatalytic activity of the samples was tested in the oxidation of phenol, chosen as model reaction. Samples were suspended (1 g/L) in phenol solution (50 ppm) in a batch reactor (200 mL) and illumination was applied through a UV-transparent Plexiglas top window (threshold absorption at 250 nm) by an Osram Ultra-Vitalux lamp (300 W) with a sun-mimicking radiation spectrum and a main emission line in the UVA range at 365 nm. The intensity of the incident UVA light on the solution was determined with a PMA 2200 UVA photometer (Solar Light Co.) being ca. 95 W/m^2. Magnetic stirring and a constant oxygen flow were used to produce a homogeneous suspension of the catalyst in the solution. Prior illumination, catalyst-substrate equilibration was ensured by stirring the suspension 20 min in the dark. The evolution of the phenol concentration was measured by UV−vis spectrometry following its 270 nm characteristic band. Total mineralization of phenol with the illumination time was followed by measuring the total organic content (TOC) in a Shimadzu 5000 TOC analyzer.

No observable changes in the initial concentration of phenol were seen in blank experiments with no catalyst, whether performed under or in the absence of illumination.

3. Results and Discussion

3.1. Characterization of Gold Sulfated and Nonsulfated Samples. The BET surface area values for sulfated and nonsulfated samples are given in Table 1. Nonsulfated materials exhibited BET surface areas of around 70 m^2/g and sulfated materials around 30 m^2/g, regardless of the gold deposition method in both cases. The lower surface areas observed for the sulfated materials likely result from the higher calcination temperature used in their preparation, despite the protection against sintering which result from sulfate pretreatment. Without the sulfate treatment, the decrease of surface area with the calcination temperature would be much higher and in fact, nonsulfated TiO_2 calcined at 700 °C presented a BET area of only 5 m^2/g, clearly demonstrating this protecting effect.

The addition of gold on the TiO_2 materials did not have any noticeable effect on the initial BET surface areas for neither of the two deposition methods.

Regarding porosity of the samples, both the sulfated and nonsulfated materials exhibited only one group of pores with an average pore diameter of 20 nm for the former and 10 nm for the latter, as shown in Table 1. Moreover, the addition of gold had no significant effect on the pore structure of the samples for any of the two deposition methods used.

XRD study of the materials revealed that only the anatase crystal form was present in both the sulfated and nonsulfated materials (XRD patterns are not provided for the sake of brevity). Previous studies have shown that pretreatment of TiO_2 with sulfuric acid both stabilizes the TiO_2 surface against sintering and inhibits conversion of the anatase crystal structure to the rutile form up to calcination temperatures as high as 700 °C.[12] It has been proposed that this stabilization results from sulfate groups which anchor to the surface of the TiO_2 precursor remaining until 700 °C.[13]

The addition of gold did not alter phase composition for any of the two series (sulfated or nonsulfated) which remained in

TABLE 1: Characterization Results

	nominal content of Au (%)	S_{BET} (m^2/g)	average pore diameter (Å)	anatase crystallite size (nm)	E_g (eV)	wt % Au (XRF)	Au atoms/nm^2
TiO_2		73	103.6	12	3.3		
S-TiO_2		31	195.2	25	3.3		
			Nonsulfated Photodeposition				
TiO_2 0.5Au PD	0.5	71	112.4	12	3.4	0.31	0.13
TiO_2 1Au PD	1	70	112.6	13	3.3	0.84	0.37
TiO_2 1.5Au PD	1.5	67	114.1	13	3.3	1.14	0.52
			Sulfated Photodeposition				
S-TiO_2 0.5Au PD	0.5	28	180.3	29	3.3	0.34	0.37
S-TiO_2 1Au PD	1	31	228.4	24	3.3	0.82	0.81
S-TiO_2 1.5Au PD	1.5	27	196.7	26	3.3	0.86	0.97
			Nonsulfated Citrate				
TiO_2 0.5Au Cit	0.5	72	104.3	13	3.3	0.39	0.17
TiO_2 1Au Cit	1	58	112.4	12	3.2	0.88	0.46
TiO_2 1.5Au Cit	1.5	64	109.7	13	3.3	1.18	0.57
			Sulfated Citrate				
S-TiO_2 0.5Au Cit	0.5	30	201.6	25	3.2	0.41	0.42
S-TiO_2 1Au Cit	1	25	244.5	27	3.3	0.81	0.99
S-TiO_2 1.5Au Cit	1.5	29	168.7	25	3.3	1.19	1.26

the anatase form in all cases. Neither the position nor the width of the peaks suffered any appreciable change, suggesting that there was not distortion of the original TiO_2 structure due to the addition of gold for any of the two deposition methods used. None of the XRD patterns displayed peaks corresponding to gold, as the metal content was below detection limit of X-ray analysis for all the samples.

Anatase crystallite sizes of the samples estimated by the Scherrer equation are also presented in Table 1. As it can be observed, sulfated materials presented sizes of 12−13 nm and nonsulfated materials sizes between 25 and 27 nm, with independence of the gold content or the deposition method used. These values are in accordance with the results of surface area obtained for the samples.

Light absorption properties were studied by UV−vis spectroscopy and the absorbance spectra of selected samples are shown in Figure 1. The values of band gap estimated for all the samples (sulfated and nonsulfated) are between 3.2 and 3.3 eV, as it can be seen in Table 1. The addition of gold did not affect significantly the absorption edge of the TiO_2 in any case. In the visible part of the spectra the surface plasmon absorption corresponding to gold can be observed with maxima around 540 nm. It has been reported that the surface plasmon resonance of gold nanoparticles may assist in the separation of photogenerated charges created in the TiO_2,[16] which could contribute to the enhancement of photocatalytic activity of some of the samples studied here, as it will be discussed later.

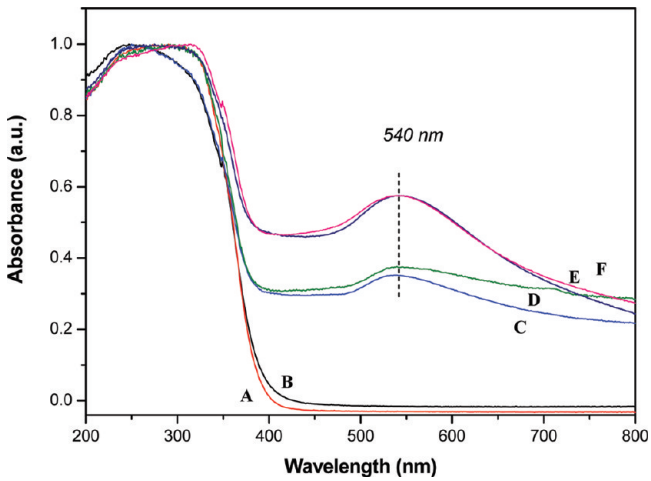

Figure 1. Absorbance spectra of selected TiO_2 samples: TiO_2 (A), S-TiO_2 (B), TiO_2 1.5Au PD (C), S-TiO2 1.5Au PD (D), TiO_2 1.5Au Cit (E), and S-TiO2 1.5Au Cit (F).

It is known that for colloidal gold nanoparticles there is a strong dependence between particle size and plasmon bandwidth and position.[16,17] The bandwidth of the surface plasmon absorption (SPA) decreases with increasing particle size for gold deposits smaller than 25 nm. The position of the absorption maximum of the SPA also depends on the particle size, with red-shifts when increasing the particle diameters for gold particles bigger than 25 nm and both red- and blue-shifts for smaller metal particles. In our case, despite the significant differences in the gold particle sizes deposited by the citrate method and by photodeposition, it can be seen in Figure 1 that the corresponding SPA do not show a marked size-sensitivity, being the plasmon bandthwith and position quite similar for both series of samples. This is probably due to the wide diameter range of the gold photodeposited particles (see TEM/SEM study below) that prevent us from appreciating any characteristic change between bands.

All samples modified by gold addition were studied by TEM and SEM to obtain information about gold deposits size and dispersion. Both techniques revealed significant differences in morphology between samples prepared by photodeposition or by citrate reduction.

TEM micrographs of selected samples are presented in Figure 2. As it can be clearly observed, photodeposition (panels A and B) led to a poor homogeneity and dispersion of gold particles, with some areas of the TiO_2 surface having a high density of gold particles and others being relatively empty. In addition, gold particles deposited via this method were irregularly sized, varying from around 10 nm to more than 100 nm in diameter.

In contrast, by deposition with the citrate method (pictures 2C and 2D), gold particles presented homogeneous spherical shape with sizes between 10−15 nm and a homogeneous dispersion on the TiO_2 surface.

When comparing sulfated samples with nonsulfated ones for both deposition methods, not important differences in the morphology of the gold particles could be observed, which was

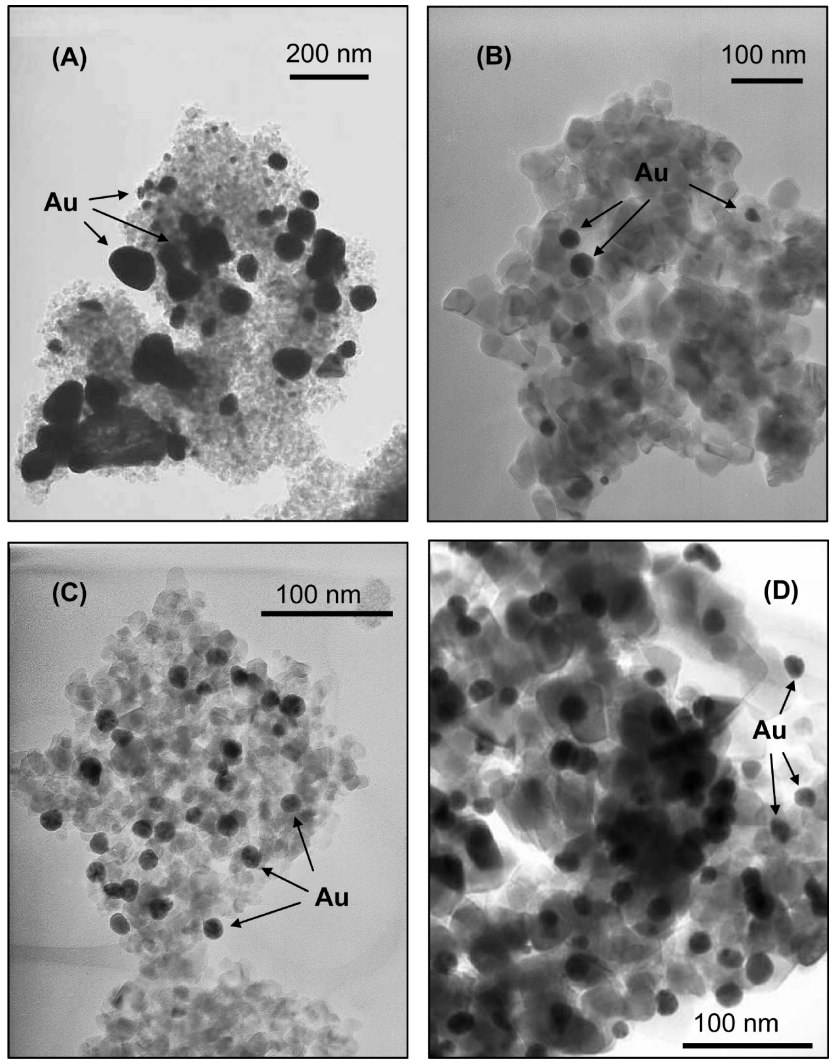

Figure 2. Transmission electron micrographs of 0.5% Au samples prepared by photodepostion onto nonsulfated TiO_2 (A) and sulfated TiO_2 (B), and 0.5% Au samples prepared by citrate reduction onto nonsulfated TiO_2 (C) and sulfated TiO_2 (D).

also confirmed by the study of the samples by SEM (selected micrographs in Figure 3).

The complete study by SEM/TEM of all the samples prepared with the different gold percentages showed that particle size and distribution did not notably change with gold content.

Total gold content in the samples was determined by XRF and the values are shown in Table 1. It was found that total content of gold was in every case a little lower than the theoretical nominal content expected for the different samples based on the quantities employed in the preparations. The final yield for gold deposition is just slightly higher for the citrate method, even if, as we have already seen in the TEM/SEM study, the morphology and size of the gold particles are very different depending on the method used.

The presence of impurities, such as Na, Cl, S, and Si, was also checked by XRF. No important amount of any of these elements was found in any of the samples. Cl content was in any case lower than 0.05 wt %, Na was found between 0.05 and 0.19 wt %, S content was always less than 0.01 wt % even in sulfated samples and Si content less than 0.05 wt %.

Since gold was incorporated into the materials by deposition with no further calcination steps subsequently carried out, it is fair to assume that the gold content measured by XRF is located entirely on the surface of the TiO_2. If we consider the surface area of the samples (Table1) and the total amount of gold on the TiO_2 surface given by XRF, the number of atoms of gold per surface area unit can be calculated and the values are shown in Table 1. This assumes too that gold particles are disposed homogenously on the TiO_2 surface, which from the observations made by TEM/SEM seems to be a good assumption for materials prepared by the citrate method but less so for materials prepared by photodeposition. Despite this limitation, these values can still provide useful information. The density of gold atoms on the surface appears to be higher when deposition is made by citrate reduction for all gold loadings and both sulfated and nonsulfated materials. Due to their surface areas, sulfated materials had higher densities than their nonsulfated counterparts.

Table 2 shows a summary of the data collected by XPS studies of the samples. Binding energies observed for Ti $2p_{3/2}$ peaks at around 458.5 eV can be assigned to Ti^{4+} in the TiO_2 lattice. In all of the samples, the O(1s) peak was observed at binding energies of around 530.0 eV and can be assigned to lattice oxygen. A small shoulder on the main peak at approximately 532 eV was also observed in all the samples, which can be associated to oxygen as surface hydroxyl groups as well as carbonate species.[18]

Moreover, XPS results also showed that in sulfated TiO_2, the ratio O/Ti is 1.70, implying that within the ca. 4 nm thickness analyzed by the XPS technique the ratio of these species is well below the stoichiometric value. This indicates the presence of

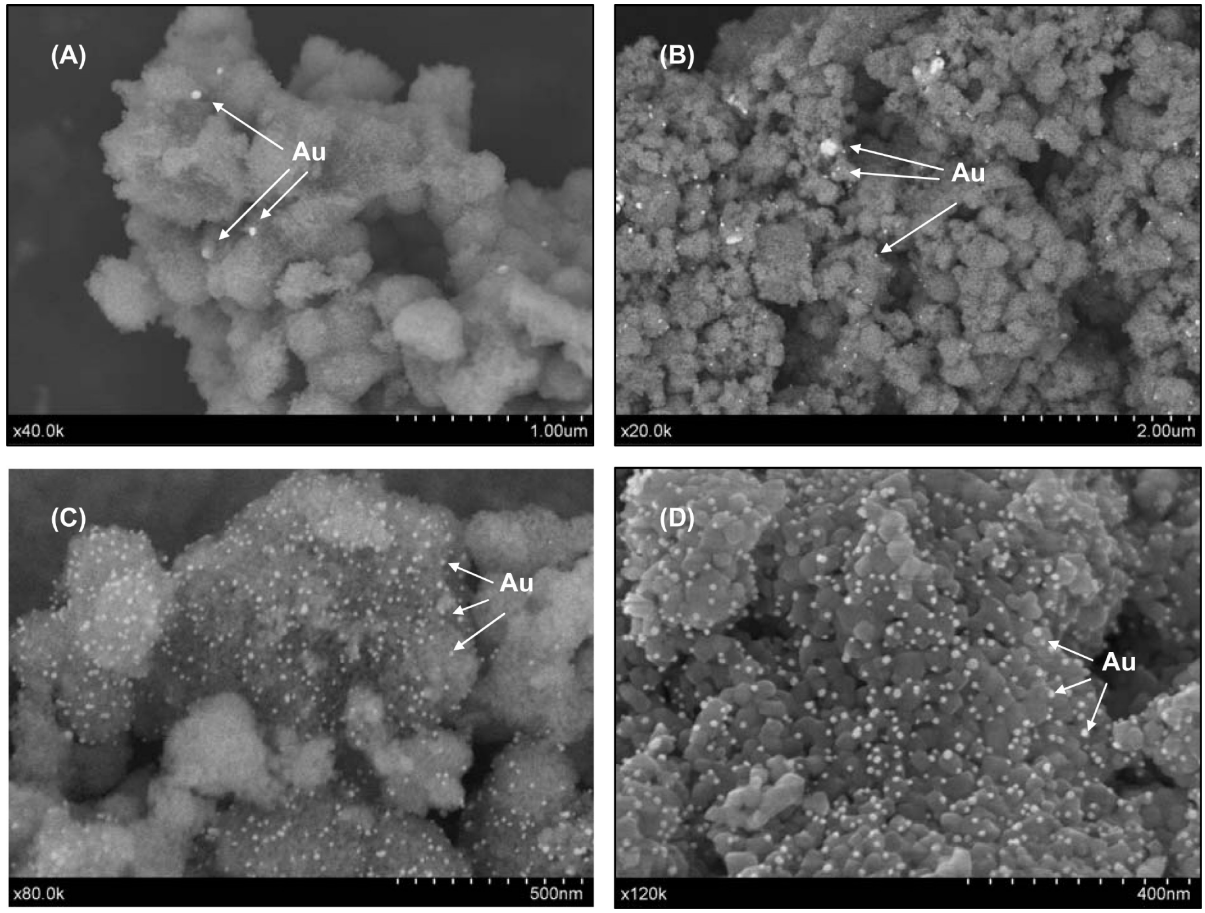

Figure 3. Scanning electron images of 1.5% Au samples prepared by photodepostion: onto nonsulfated TiO_2 (A) and sulfated TiO_2 (B), and 1.5% Au samples prepared by citrate reduction onto: nonsulfated TiO_2 (C) and sulfated TiO_2 (D).

TABLE 2: Summary of XPS Results for the Different Samples

	Binding Energy (eV)		XPS Au (at.%)	XPS intensity ratios I_{Au}/I_{Ti}
	Ti $2p_{3/2}$	O 1s		
TiO_2	458.6	530.1		
S-TiO_2	458.6	530.2		
Nonsulfated Photodeposition				
TiO_2 0.5Au PD	458.5	530.2	0.08	0.008
TiO_2 1Au PD	458.5	529.8	0.09	0.014
TiO_2 1.5Au PD	459.3	530.9	0.12	0.027
Sulfated Photodeposition				
S-TiO_2 0.5Au PD	458.4	529.7	0.07	0.011
S-TiO_2 1Au PD	458.5	529.8	0.13	0.019
S-TiO_2 1.5Au PD	458.5	530.2	0.13	0.022
Nonsulfated Citrate				
TiO_2 0.5Au Cit	458.6	530.1	0.15	0.019
TiO_2 1Au Cit	458.1	529.7	0.32	0.057
TiO_2 1.5Au Cit	458.5	529.8	0.55	0.070
Sulfated Citrate				
S-TiO_2 0.5Au Cit	458.3	529.7	0.15	0.022
S-TiO_2 1Au Cit	457.8	529.1	0.35	0.061
S-TiO_2 1.5Au Cit	458.5	529.8	0.37	0.103

a certain number of oxygen vacancies in the surface of the material. The amount of these vacancies should be much lower in the nonsulfated TiO_2 samples as a O/Ti ratio close to the stoichiometric value (O/Ti = 2) was observed, in agreement with previous results reported by some of us.[13] The vacancies in the sulfated materials should result from the dehydroxylation of excess adsorbed protons during the final stage of sulfate elimination when the materials are calcined at 700 °C.

For all sulfated samples, no signal was detected in XPS analysis of the S(2p) region, indicating that the amount of S on the surface of these samples is negligible. These results show that for sulfated samples all sulfate groups were removed during their calcination at 700 °C, in accordance with previous observations.[12]

The determination of the nature and oxidation state of the Au species (Au^0, Au^I and Au^{III}) can also be accomplished by XPS by means of the Au 4f peak study. Figure 4 shows the Au (4f) region for some selected samples (prepared by photodeposition or citrate method and sulfated or nonsulfated). The Au 4f region is characterized by a doublet corresponding to Au $4f_{7/2}$ and Au $4f_{5/2}$ with a separation of about 3.7 eV. In the samples the main Au $4f_{7/2}$ component is located at a binding energy of 83.0−83.1 eV which can be assigned to metallic gold Au^0, with the corresponding Au $4f_{5/2}$ peaks appearing at 86.6−86.8 eV. No peaks or shoulders can be observed at higher binding energies in the spectra and therefore no oxidized surface gold species are expected on the surface of any of the samples (Au^I $4f_{7/2}$ at 84.5 eV and Au^{III} $4f_{7/2}$ at 85.6 eV). Figure 4 shows only the spectra of the 1.5% Au samples, but same conclusions can be reached for the materials with other gold contents (spectra not shown). From these results we can conclude that for both deposition methods the reduction of gold has been completed and gold is present only in its metallic form, Au^0, with no detectable contribution of Au^I or Au^{III}.

The oxidation state of gold on the TiO_2 surface is very important in photocatalytic terms; gold particles of the sizes observed in the materials studied here enhance the photocatalytic activity by means of their capacity to form a Schottky junction

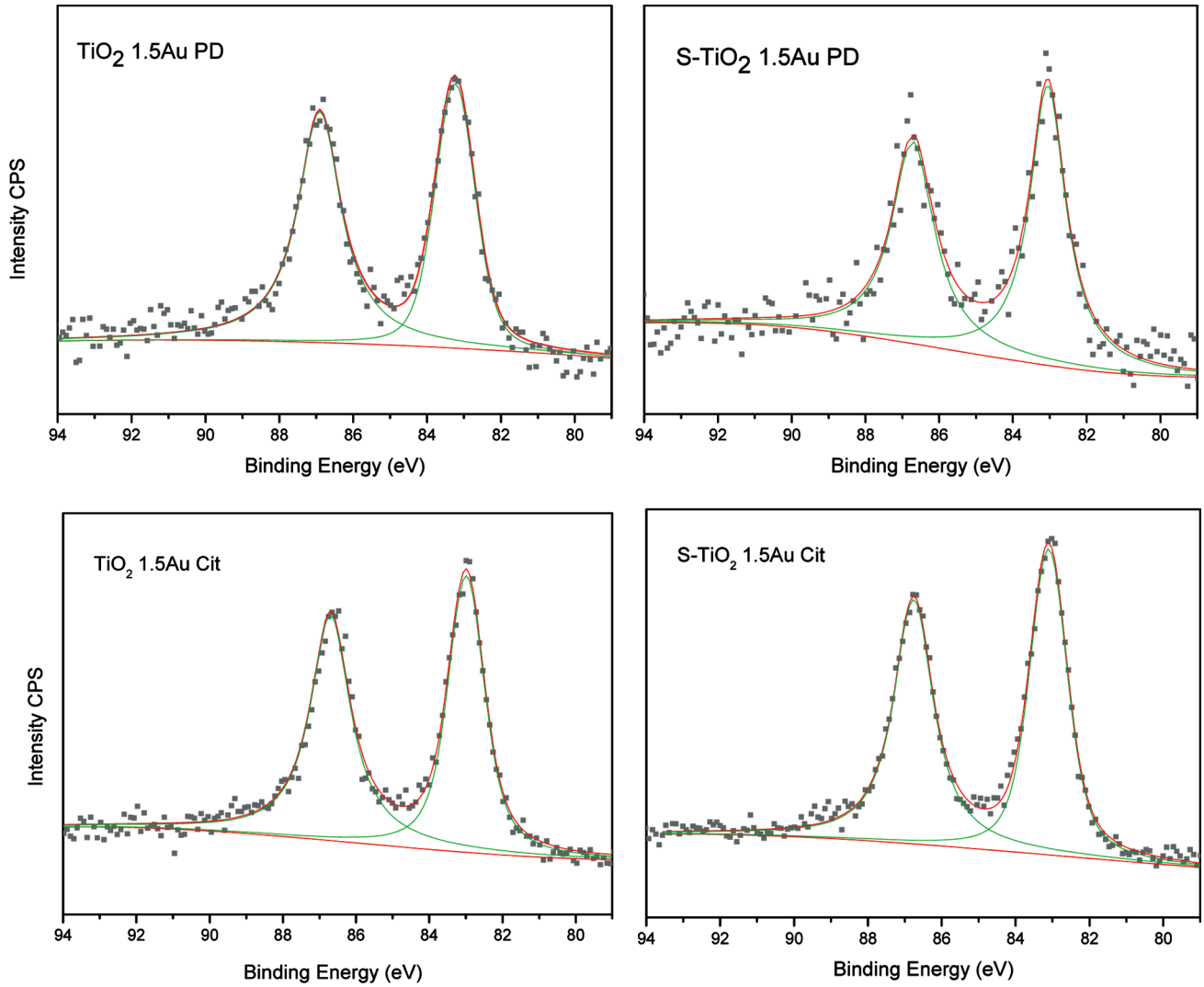

Figure 4. XPS spectra in the Au 4f region for the specified samples.

with the TiO_2. The metal particles may thus act as sinks for photogenerated electrons, reducing the recombination rate of the generated charges.[8,19] It is important therefore that the deposited gold is metallic in order to allow this mechanism of enhancement.

XPS is a surface sensitive technique which also gives information about how well particles are dispersed over a support.[20] The XPS study of our samples can provide us useful information for comparing gold particle size and dispersion resulting from the two different deposition methods. For two samples with the same total amount of gold, the sample with a higher dispersion of the metal on the surface will show a higher signal peak for gold related to the signal of titanium, and consequently a high ratio of intensities I_{Au}/I_{Ti} in the XPS spectrum because the corresponding TiO_2 surface will be more largely covered. Thus, the XPS intensity ratio I_{Au}/I_{Ti} can reflect the dispersion of gold on the TiO_2. Figure 5 plots the ratio of XPS intensities I_{Au}/I_{Ti} versus the nominal amount of gold on the different samples. In this graphic, two different trends can be clearly differentiated, on one side samples prepared with the photodeposition method (TiO_2 PD and S-TiO_2 PD) and on the other side samples prepared by the citrate method (TiO_2 Cit and S-TiO_2 Cit). The steeper gradients observed as gold loading is increased for samples prepared by citrate reduction indicate that this method gives smaller, better dispersed gold particles, regardless of whether the TiO_2 was sulfated or not. These results

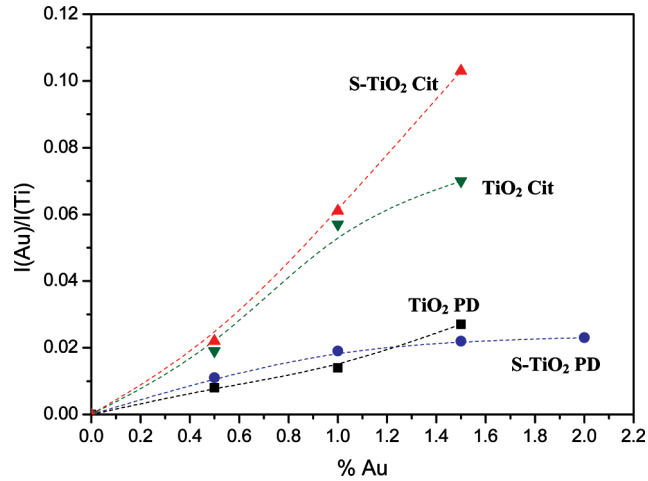

Figure 5. Relative XPS intensity for Au(4f) as a function of nominal gold loading for nonsulfated TiO_2/photodepostion (TiO_2 PD), sulfated TiO_2/photodepostion (S-TiO_2 PD), nonsulfated TiO_2/citrate method (TiO_2 Cit) and sulfated TiO_2/citrate method (S-TiO_2 Cit).

confirm the conclusions reached by the study by TEM/SEM regarding gold particle size and dispersion.

Nevertheless, in this kind of study, it is also important to take into account the surface areas of the samples, which in

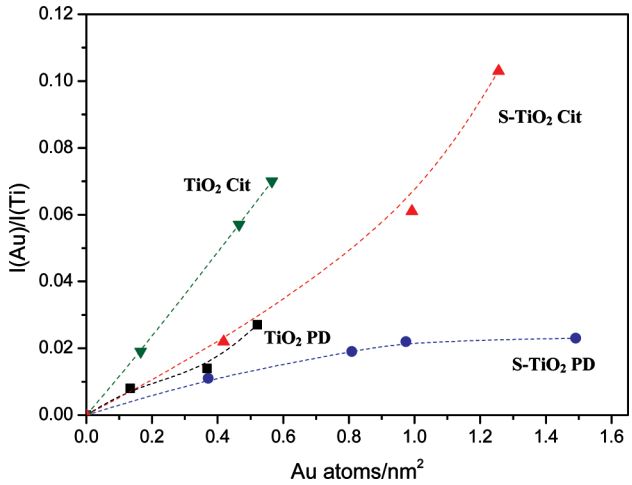

Figure 6. Relative XPS intensity for Au(4f) as a function of the surface concentration of gold for nonsulfated TiO_2/photodepostion (TiO_2 PD), sulfated TiO_2/photodepostion (S-TiO_2 PD), nonsulfated TiO_2/citrate method (TiO_2 Cit) and sulfated TiO_2/citrate method (S-TiO_2 Cit).

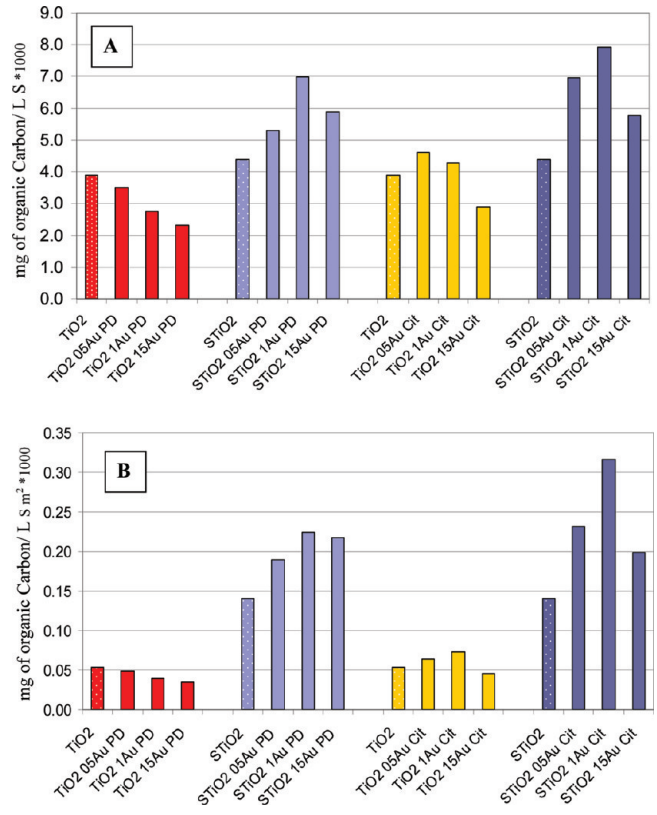

Figure 7. Initial reaction rates for phenol mineralization (mg of organic carbon eliminated per liter and second) over the indicated catalysts (A) and normalized per surface area unit of catalyst (mg of organic carbon eliminated per liter, second and m^2) (B).

our case are very different for sulfated and not sulfated series (Table 1). To normalize the different areas of the samples, Figure 6 depicts the relative XPS intensities (I_{Au}/I_{Ti}) as a function of the surface concentration of gold on the different materials (Au atoms per surface unit). For a same metal loading per surface area unit, a higher XPS intensity I_{Au}/I_{Ti} ratio implies a better dispersion of the metal on the TiO_2 surface. Therefore, the larger the slope representing a series of samples the more dispersed is the metal.[21] In Figure 6 the better dispersions are clearly found for the materials prepared by the citrate method. Through this normalization it becomes clear that the nonsulfated materials exhibit higher dispersion than the sulfated ones. This is to be expected due to the higher surface areas of the former materials, where the metal can spread on a higher extent. The higher tendency for gold particle aggregation in samples prepared by photodeposition is reflected by the leveling on the slope of XPS intensity ratios at high gold loading corresponding to this series (see S-TiO_2 PD in Figure 6). This is not observed in materials prepared by the citrate reduction method (see S-TiO_2 Cit in Figure 6).

The results obtained from XPS studies presented in Figures 5 and 6, together with the observations made by TEM/SEM, demonstrate significant differences in the morphology of the deposited gold particles (size, shape and dispersion) depending on whether gold deposition was by photodeposition or by citrate reduction. On the contrary, no important differences could be found between sulfated and not sulfated samples, if the same deposition method was used. The higher dispersion observed for the nonsulfated materials is merely a consequence of their higher surface areas.

3.2. Photocatalytic Activity. Photocatalytic activity of the Au-TiO_2 samples, sulfated and nonsulfated, was evaluated following the reaction of phenol photo-oxidation. Phenol concentration was measured by UV−vis spectrometry following its 270 nm characteristic band and the total mineralization of phenol was estimating by measuring the total organic content (TOC) with the illumination time. The different activities of all samples were estimated by taking the initial slope (30 min) of TOC disappearance (mg TOC s^{-1} L^{-1}) with the illumination time, represented in Figure 7A and normalized per unit area of catalyst (mg TOC s^{-1} L^{-1} m^{-2}) in Figure 7B. It can be observed that for the nonsulfated samples the activity of the samples for phenol degradation increases very slightly (citrate method) or even clearly decreases (photodeposition) with the addition of gold. On the contrary, for sulfated samples the activity increases with gold addition, especially for the citrate method, with a maximum at 1% gold content for both deposition methods. This trend becomes more apparent when the activity is normalized with respect to the surface areas of the catalysts (Figure 7B). Thus, we can find a clear difference in the photocatalytic behavior between the sulfated and the nonsulfated catalysts. The best photocatalytic activity is shown by the sulfated samples prepared by the citrate method.

For reference purposes and to justify the reasons for choosing different calcination temperatures for the sulfate and the non sulfate series, sulfated TiO_2 was also calcined at 500 °C rather than 700 °C. The photocatalytic activity of this sample is quite low compared to the same sample calcined at 700 °C, also after 1 wt % Au addition by the citrate method, despite the much higher surface areas (ca. 120 m^2/g). Nonsulfated TiO_2 calcined at 700 °C loses nearly all of its surface area (S_{BET} = 5 m^2/g) and shows hardly any photocatalytic activity.

The enhancement in the photocatalytic activity of TiO_2 by the surface deposition of gold nanoparticles has been ascribed to an improvement of charge separation. The metal particles act as sinks for the photogenerated electrons, which reduces charge recombination and consequently increases the efficiency of the photocatalytic process.[8,19] In this promoting effect, size and dispersion of gold particles as well as effectiveness of the electronic communication between the metal and the TiO_2 are very important factors to take into account.[19,22]

Characterization of the materials showed that the citrate reduction method resulted in smaller, more evenly dispersed nanoparticles than the photodeposition method. Clearly, this serves to explain the greater increase in activity resulting from

gold deposition in samples prepared by the former method compared to the latter (Figure 7). Smaller and homogenously distributed gold particles on the TiO_2 surface of samples prepared by the citrate method can act as much effective traps for photogenerated electrons. Moreover, for the nonsulfated samples prepared by photodeposition the activity decreases with the addition of gold, probably due to the shadowing and blocking of TiO_2 active sites by the big and scarcely effective gold particles in these samples.

The increase of activity with the addition of gold is notably higher for samples which have been previously sulfated. This difference in the activity behavior cannot be justified by reasons of particle size and dispersion since sulfated and nonsulfated samples present similar gold particle sizes as it has been shown in the characterization section.

Mohapatra et al. found recently an important increase in the activity of gold/titania catalysts for room-temperature oxidation of CO by sulfate pretreatment of the oxide.[23] These authors attributed the promotional effect to a direct interaction between sulfate ions with the gold atoms, as their samples were calcined at only 400 °C and still retained high amount of sulfate groups on the surface. However, in our case there are not remaining sulfate groups on the TiO_2 surface after calcination at 700 °C as it was confirmed by XPS and a different mechanism must be responsible for the enhancement of activity.

Okazaki et al. proved by density functional studies that the adhesive energies between Au and TiO_2 for nonstoichiometric surfaces were much larger than those on stoichiometric surfaces and that charge transfer between the gold and the oxide is more effective on Ti-rich surfaces, e.g., on nonstoichiometric or defect rich surfaces.[24,25] Vittadini and Selloni reached similar conclusions for small gold clusters on defected anatase TiO_2.[26] In our case, sulfated samples were found to have a highly defected surface, determined by their low XPS O/Ti ratios. It is likely that this strengthens the adsorption of Au onto the vacant oxygen sites, at which gold tends to adsorb on reduced surfaces, increasing the extent and effectiveness of the electronic communication between gold and the TiO_2 surface. This would increase the efficiency of charge separation and thus, the efficiency of the photocatalytic processes.

4. Conclusions

Significant increases in the photocatalytic activity of TiO_2 were achieved by surface deposition of gold nanoparticles on materials pretreated with sulfate and then subjected to high temperature calcination (700 °C). This sulfate pretreatment did not influence the average size of the gold particles and their dispersion. The much higher improvement in the activity of presulfated samples compared to nonsulfated ones is ascribed to the stronger bonding and superior electronic junction between the gold particles and the TiO_2 surface on the more highly defective surfaces of the sulfated materials.

Moreover, two different methods of gold addition were compared; photodeposition and chemical reduction by citrate. These two methods were found to lead to very different morphologies and average particle sizes and shapes of gold particles. The citrate method gave much homogeneous and smaller gold particles with a better dispersion than photodeposition. For these reasons, samples prepared by the citrate reduction method exhibited greater improvements in activity in the photocatalytic degradation of phenol with the addition of gold for both sulfated and nonsulfated materials.

In this work, it has been shown that gold addition by the citrate method on presulfated TiO_2 is a good procedure for obtaining gold particles of homogeneous particle size and dispersion with a strong bonding and interaction between the gold particles and the TiO_2 surface. This system appears to have excellent properties for photocatalytic applications and could also hold much potential if extended to other areas of catalysis by supported gold.

Acknowledgment. This research was financed by the Spanish Ministerio Ciencia e Innovación (Project Ref CTQ2008-05961-CO2-01). Financial support by Junta de Andalucía (P.A.IDI group FQM181 annual funding and Excellence Project P06-FQM-1406) is also acknowledged. The authors thank Dr. María Jesús Sayagues for her assistance with the transmission electron microscopy.

References and Notes

(1) Overbury, S. H.; Schwartz, V.; Mullins, D. R.; Yan, W.; Dai, S. *J. Catal.* **2006**, *241*, 56.
(2) Romero-Sarria, F.; Martínez, L. M.; Centeno, M. A.; Odriozola, J. A. *J. Phys. Chem. C* **2007**, *111*, 14469.
(3) Gluhoi, A. C.; Bogdanchikova, N.; Nieuwenhuys, B. E. *J. Catal.* **2005**, *232*, 96.
(4) Kim, C. H.; Thompson, L. T. *J. Catal.* **2005**, *230*, 66.
(5) Iliev, V.; Tomova, D.; Todorovska, R.; Oliver, D.; Petrov, L.; Todorovsky, D.; Uzunova-Bujnova, M. *Appl. Catal., A* **2006**, *313*, 115.
(6) Li, H.; Bian, Z.; Zhu, J.; Huo, Y.; Li, H.; Lu, Y. *J. Am. Chem. Soc.* **2007**, *129*, 4538.
(7) Tian, B.; Zhang, J.; Tong, T.; Chen, F. *Appl. Catal., B* **2008**, *79*, 394.
(8) Subramanian, V.; Wolf, E. E.; Kamat, P. V. *J. Am. Chem. Soc.* **2004**, *126*, 4943.
(9) Mrowetz, M.; Villa, A.; Prati, L.; Selli, E. *Gold Bull.* **2007**, *40*, 154.
(10) Hidalgo, M. C.; Maicu, M.; Navío, J. A.; Colón, G. *Catal. Today* **2007**, *129*, 43.
(11) Hidalgo, M. C.; Maicu, M.; Navío, J. A.; Colón, G. *Appl. Catal., B* **2008**, *81*, 49.
(12) Colón, G.; Hidalgo, M. C.; Navío, J. A. *Appl. Catal., B* **2003**, *45*, 39.
(13) Colón, G.; Hidalgo, M. C.; Munuera, G.; Ferino, I.; Cutrufello, M. G.; Navío, J. A. *Appl. Catal., B* **2006**, *63*, 45.
(14) Kimling, J.; Maier, M.; Okenve, B.; Kotaidis, V.; Ballot, H.; Plech, A. *J. Phys. Chem. B* **2006**, *110*, 15700.
(15) Tandom, S. P.; Gupta, J. P. *Phys. Status Solidi* **1970**, *38*, 363.
(16) Min, B. K.; Heo, J. E.; Youn, N. K.; Joo, O. S.; Lee, H.; Kim, J. H.; Kim, H. S. *Catal. Commun.* **2009**, *10*, 712.
(17) Link, S.; El-Sayed, M. A. *J. Phys. Chem. B* **1999**, *103*, 4212.
(18) Aramendía, M. A.; Colmenares, J. C.; Marinas, A.; Marinas, J. M.; Moreno, J. M.; Navío, J. A.; Urbano, F. J. *Catal. Today* **2007**, *128*, 235.
(19) Orlov, A.; Jefferson, D. A.; Macleod, N.; Lambert, R. M. *Catal. Lett.* **2004**, *92*, 41.
(20) Chorkendorff, I.; Niemantsverdriet, J. W. *Concepts of Modern Catalysis and Kinetics*; Wiley-VCH Verlag: Weinheim, Germany, 2003.
(21) Gonzalez-Elipe, A. R.; Munuera, G.; Espinos, J. P. *Surf. Interface Anal.* **1990**, *16*, 375.
(22) Iliev, V.; Tomova, D.; Bilyarska, L.; Tyuliev, G. J. *Mol. Catal. A* **2007**, *263*, 32.
(23) Mohapatra, P.; Moma, J.; Parida, K. M.; Jordaan, W. A.; Scurrell, M. S. *Chem. Commun.* **2007**, 1044.
(24) Okazaki, K.; Morikawa, Y.; Tanaka, S.; Kohyama, M. *Phys. Rev. B* **2004**, *69*, 235404.
(25) Okazaki, K.; Morikawa, Y.; Tanaka, S.; Tanaka, K.; Kohyama, M. *J. Mater. Sci.* **2005**, *40*, 3075.
(26) Vittadini, A.; Selloni, A. *J. Chem. Phys.* **2002**, *117*, 353.

JP903432P